Non-Invasive Characterization of Atrial Fibrillation Based on Multiscale Analysis of Body Surface Potential Mapping

Marina B Conesa-Peraleja[1], Miriam G Fernández[1,3], Karen L Linares[3,4], Carlos F Santos[2], María S Guillem[2], Andreu M Climent[2], Óscar B Pérez[1]

[1]Universidad Rey Juan Carlos, [2]ITACA Institute, Universitat Politècnica de València, Spain
[3]Vicomtech, Basque Research and Technology Alliance, [4]eHealth Group, Biogipuzkoa Institute

Abstract

Atrial Fibrillation (AF) is the most common cardiac arrhythmia, linked to increased risk of stroke, heart failure, and mortality poses a serious health challenge. This work proposes a noninvasive method to characterize Body Surface Potential Maps (BSPMs) of varying complexity using the Wavelet Scattering Transform (WST). The goal is to distinguish between normal sinus rhythm, AF with fibrosis, and AF with multiple rotors through a classification framework. The processing pipeline includes dimensionality reduction via PCA, robust time-frequency feature extraction using WST, and classification with a Random Forest model. The best results were achieved on dataset with noise injection of 10 dB SNR, reaching 99.6% accuracy. Misclassification analysis indicated that spectral overlap, particularly in cases with interacting rotors, can hinder class separation. These results support the potential of WST-based BSPM analysis for noninvasive AF mechanism characterization.

1. Introduction

Atrial fibrillation (AF) is the most prevalent sustained arrhythmia worldwide, affecting more than 33 million people and associated with significant morbidity and mortality, representing a major health challenge [1, 2]. Current treatment strategies include antiarrhythmic drugs and catheter ablation. Successful ablation depends on the precise identification of arrhythmic drivers, such as focal sources or rotors, typically using electroanatomical mapping systems [3]. However, these systems are invasive, time-consuming, and limited by their non-global perspective, which hinders the detection of complex and dynamic atrial activity [4].

Electrocardiographic Imaging (ECGI) is a noninvasive alternative that reconstructs epicardial potentials from Body Surface Potential Maps (BSPMs) and anatomical models from computed tomography scans. BSPMs, recorded from high-density electrode arrays, provide spatially rich representations of cardiac activity [5]. Despite their potential to reflect intracavitary activity, BSPMs are high-dimensional, noisy, and nonstationary. Standard signal processing techniques such as the Fourier Transform or Short-Time Fourier Transform struggle to extract localized transient patterns relevant to AF [6]. In contrast, the **Wavelet Scattering Transform** (WST) provides translation-invariant time-frequency features that are robust and informative [7].

Recent studies have applied AI to BSPMs for noninvasive arrhythmia characterization. Deep learning models, including CNNs and hybrids, have achieved high accuracy in AF recurrence prediction and ECG inverse problem solving using both simulated and clinical data [8, 9]. Classical approaches combining wavelet-based features with machine learning also performed well [10], and recent use of the WST in ECG rhythm classification has shown promising results with neural networks [11, 12], highlighting the value of wavelet features in AF analysis.

The aim of this study is to characterize BSPMs of varying electrophysiological complexity using the WST, facilitating the noninvasive differentiation of atrial activation patterns, namely, normal sinus rhythm, AF with fibrosis, and AF presenting multiple rotors, through a multiclass classification framework. To achieve this, a processing pipeline was developed combining dimensionality reduction using Principal Component Analysis (PCA), robust time-frequency feature extraction via WST, and classification using a Random Forest (RF) machine learning model.

This manuscript is structured as follows: Section 2 presents the methods, followed by the results in Section 3, and concluding remarks in Section 4.

2. Methods

2.1. Dataset

A dataset of simulated BSPMs, generated from realistic atrial models by solving the forward problem of electrocardiography through computational simulations of EGM signals, as described in [13], was used. To solve the forward

problem, ten different torso geometries were employed, and BSPM models were generated by linearly combining these torso structures with the EGM computational models. Each BSPM model contains 64-lead surface potentials sampled at 500 Hz.

This dataset, containing data from 52 individuals, was categorized into three classes based on the complexity of atrial activation wavefronts: (Class 0) 13 models exhibited Normal Sinus Rhythm, (Class 1) 8 corresponded to AF characterized by fibrosis and rotors, and (Class 2) 31 displayed AF exhibiting multiple rotors (but no fibrosis).

To standardize the signal length in the dataset to 2000 samples, only models with at least this length were considered. Longer signals were truncated accordingly, except those of exactly 4000 samples, which were split into two equal segments, each covering at least two heartbeats.

2.2. Experimental Set-Up

From this baseline dataset, four variants datasets were generated for comparative evaluation:

- **Original with PCA**: Raw BSP signals without added noise. PCA was applied at each BSPs signal, across the 64 electrodes, to retain the most significant spatial components. The number of components was selected based on cumulative explained variance in the training set.
- **Filtered 10 dB**: Signals with added Gaussian white noise (10 dB SNR) followed by a 40 Hz low-pass (LP) filter applied. PCA was applied as in previous variant.
- **Filtered 20 dB**: Signals with added Gaussian white noise (20 dB SNR) followed by a 40 Hz LP filter applied. PCA was applied as in previous variants.
- **Original (No PCA)**: Original signals processed without applying PCA prior to feature extraction.

In each dataset, a WST using Morlet wavelets was applied to extract first-order and second-order time-frequency coefficients, generating translation-invariant features robust to deformations and noise.

These features were then used to train a RF classifier, independently for each dataset. To ensure unbiased evaluation, the data were split at the individual level, keeping all versions of each individual EGM signal in the same partition, resulting in 560 training samples and 250 test samples.

2.3. Classification and Evaluation

A RF classifier was used for the classification task. RF is a supervised ensemble method that combines multiple decision trees, each trained on a random subset of the data and features. Predictions are made by majority voting among the trees, improving generalization and reducing overfitting through bootstrapping and feature randomness [14, 15].

Hyperparameters used in the models were optimized via randomized search with 5-fold cross-validation (50 iterations) using accuracy as the metric. Tuning was performed separately for each dataset, and the number of trees was not included in the search, but it was fixed to 250.

2.4. Evaluation Metrics

Evaluation metrics were computed to assess classification performance by comparing predicted versus ground truth classes. The following metrics were used:

- **Accuracy**: Overall proportion of correct predictions.
- **Sensitivity (Recall)**: Proportion of correctly identified AF cases.
- **Specificity**: Proportion of correctly identified NSR cases.
- **Precision**: Proportion of positive predictions that were correct.
- **F1-score**: Harmonic mean of precision and sensitivity.
- **AUC-ROC**: Area under the ROC curve, indicating the model's discrimination capacity.
- **Log-loss**: Penalizes incorrect predictions made with high confidence.

3. Results

The RF classifier achieved strong performance across all tested data subsets, successfully differentiating between sinus rhythm, AF with fibrosis, and AF with multiple rotors, as detailed in Table 1. The highest accuracy (0.996) was achieved with subset 10 dB SNR and LP filtered, suggesting that moderate noise may act as a regularizer, improving model generalization. The confusion matrix and the average and individual ROC curves for this model are shown in Figure 2.

Metric	Original	Filtered 10 dB	Filtered 20 dB	Original (No PCA)
Accuracy	0.960	0.996	0.968	0.960
F1 Score	0.963	0.996	0.970	0.963
Sensitivity	0.982	0.998	0.986	0.982
Specificity	0.889	0.984	0.905	0.889
AUC-ROC	0.975	0.999	0.999	0.981
Log Loss	0.148	0.098	0.076	0.133

Table 1: Performance metrics for the RF classifier across different data subsets.

Applying PCA prior to WST did not yield a noticeable improvement in performance, suggesting that WST is inherently robust to input dimensionality and capable of extracting discriminative features without prior dimensionality reduction. Nevertheless, this step substantially reduced the computational cost, making it a valuable preprocessing option even when classification accuracy remains unchanged.

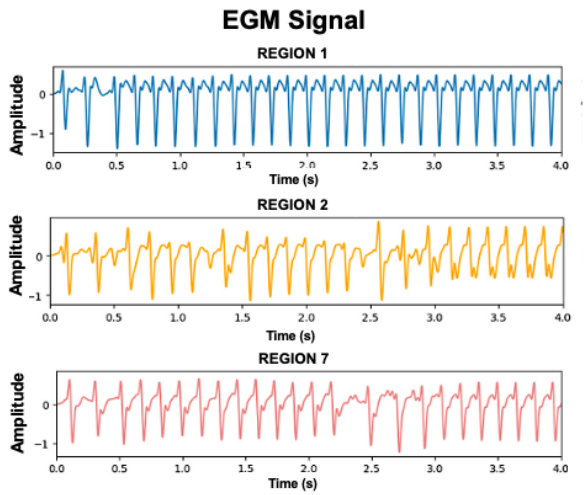

(a) EGMs recorded from atrial regions 1 (blue), 2 (yellow), and 7 (red).

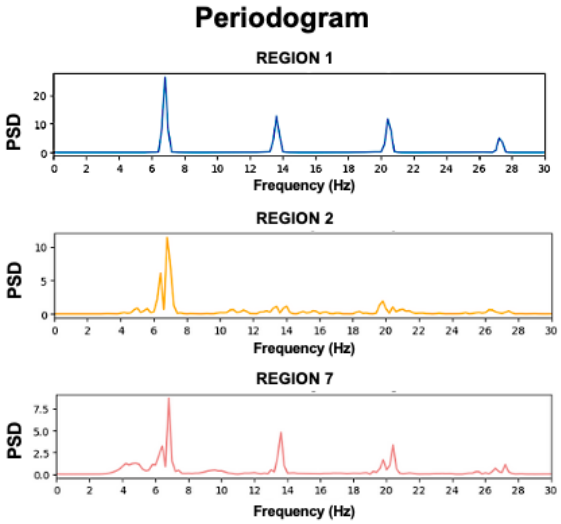

(b) Corresponding periodograms illustrating frequency components of the EGMs shown above.

Figure 1: Representative EGM signals and their spectral profiles in a misclassified AF case with multiple rotors.

To explore the classifier's limitations, misclassified BSPM signals, especially AF with Multiple Rotors predicted as AF with Fibrosis, were analyzed in time and frequency domains. These errors likely stem from overlapping spectral features and shared surface-level characteristics. Further analysis at the EGM level revealed that rotor regions showed regular activation with dominant frequencies, while the collision zone of rotors exhibited irregular, broadband activity as shown in Figure 1. This local disruption likely distorted the BSPM, introducing ambiguous patterns that hindered correct classification. These findings highlight the challenge posed by spatiotemporal complexity in AF and suggest that rotor interactions should be better addressed in future models.

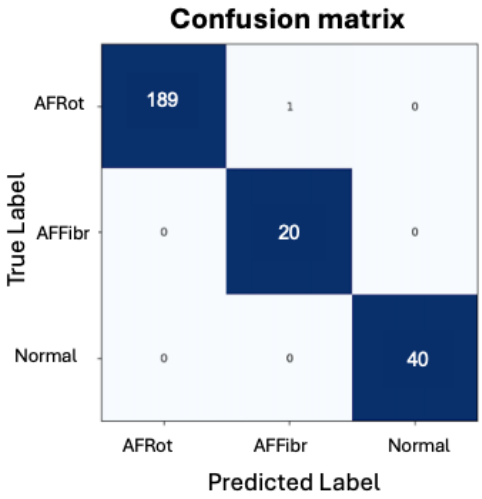

(a) Confusion matrix showing prediction accuracy across three classes: normal sinus rhythm (Normal), AF with fibrotic activity (AFFibr), and AF with multiple rotors (AFRot).

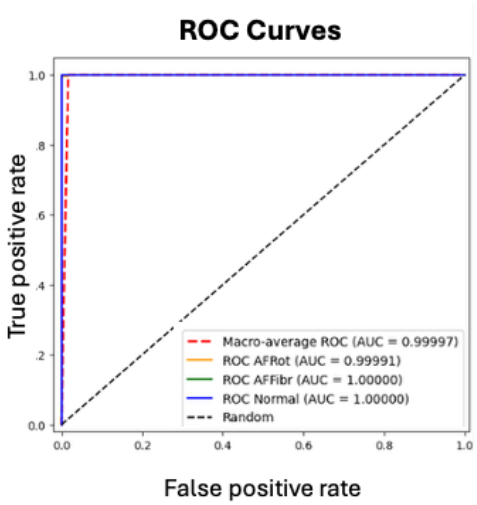

(b) Receiver Operating Characteristic (ROC) curves for each class, demonstrating the model's discrimination capability.

Figure 2: Confusion matrix and ROC curves obtained for the RF classifier for the 10 dB filtered dataset, the dataset that delivers the best performing model for each class: AF with more than two rotors (AFRot), AF with fibrotic activity (AFFibr), and normal sinus rhythm (Normal).

4. Conclusions

This work presents a methodology to characterize BSPMs of varying electrophysiological complexity using the WST. By combining PCA for dimensionality reduc-

tion, WST for robust time-frequency feature extraction, and RF classification, the system effectively distinguished between sinus rhythm, AF with fibrosis, and AF with multiple rotors. The best performance was achieved on data with 10 dB SNR and LP filtering, reaching 99.6% accuracy, demonstrating strong robustness to noise and preprocessing variations. Misclassifications were mainly linked to overlapping spectral features in rotor-interaction regions. Overall, the results support WST as a powerful tool for noninvasive characterization of atrial activation patterns.

Future work should explore real patient data, more complex rhythm types, and integration of spatial information to enhance clinical relevance and guide mechanism-targeted therapies.

Acknowledgments

This work has been partially supported by: Ministerio de Ciencia (PID2019-105032GB-I00, PID2022-136887NB-I00), Universidad Rey Juan Carlos (2023/00004/006-F918), Instituto de Salud Carlos III, and Ministerio de Ciencia, Innovación y Universidades (supported by FEDER Fondo Europeo de Desarrollo Regional PI17/01106 and RYC2018-024346B-750), Consejería de Ciencia, Universidades e Innovación of the Comunidad de Madrid through the program RIS3 (S-2020/L2-622), EIT Health (Activity code 19600, EIT Health is supported by EIT, a body of the European Union) and the European Union's Horizon 2020 under the Marie Skłodowska-Curie grant agreement No. 860974.

References

[1] Gómez-Doblasa J, López-Garrido M, Esteve-Ruiz I, Barón-Esquivias G. Epidemiología de la fibrilación auricular. Rev Esp Cardiol Supl 2016;16A:2–7.

[2] Elliott A, Middeldorp M, Van Gelder I, Albert C, Sanders P. Epidemiology and modifiable risk factors for atrial fibrillation. Nat Rev Cardiol 2023;20(6):404–417.

[3] Sagris Mea. Atrial fibrillation: Pathogenesis, predisposing factors, and genetics. Int J Mol Sci 2021;23(1):6.

[4] de Groot N, Shah D, Boyle P, Anter E, Clifford G, et al. Critical appraisal of technologies to assess electrical activity during atrial fibrillation. Europace 2022;24(2):313–330.

[5] Intini A, Goldstein R, Jia P, Ramanathan C, et al. Ecgi used for mapping focal lv tachycardia. Heart Rhythm 2005; 2(11):1250–1252.

[6] Xia Y, Wulan N, Wang K, Zhang H. Detecting atrial fibrillation by deep convolutional neural networks. Comput Biol Med 2018;93:84–92.

[7] Lee D, Yamamoto A. Wavelet analysis: Theory and applications. Hewlett Packard J 1994;45(Dec).

[8] Li Z, Yang C, Zhang Q. Noninvasive prediction of af recurrence via deep learning. In Proc. 2nd Int. Conf. Comput. Biol. Bioinf. (ICBB). 2018; 67–71.

[9] Chang Y, Dong M, Fan L, et al. Noninvasive ep imaging via dl and cardiac simulation. BMC Cardiovasc Disord 2025; 25(1):335.

[10] Marques V, Rodrigo M, Guillem M, Salinet J. Characterization of atrial arrhythmias in bspm: A computational study. Comput Biol Med 2020;127:103904.

[11] Bourkha M, Hatim A, Nasir D, Beid S. Af detection via wst and neural networks. Int J Adv Comput Sci Appl 2023;14.

[12] Marzog H, Abd H. Machine learning ecg classification using wavelet scattering of feature extraction. Appl Comput Intell Soft Comput 2022;2022(1):9884076.

[13] Rodrigo M, Climent A, Liberos A, et al. Technical considerations on phase mapping for atrial reentrant activity. Circ Arrhythm Electrophysiol 2017;10(9):e005008.

[14] Breiman L. Random forests. Mach Learn 2001;45(1):5–32.

[15] Salman H, Kalakech A, Steiti A. Random forest algorithm overview. Babylonian J Mach Learn 2024;2024:69–79.

Address for correspondence:

Marina Burgos Conesa-Peraleja
28006 Madrid, Spain
marinaburgosc2@gmail.com